A Comparison of FPS-16 and GMD-1 Measurements and Methods for Processing Wind Data

E. F. DANIELSEN[1] AND R. T. DUQUET

The Pennsylvania State University, University Park

(Manuscript received 24 June 1966, in revised form 19 June 1967)

ABSTRACT

A machine method for computing winds from radiosonde and GMD-1 rawin tracking data is developed and the resulting winds are compared to those computed from precision FPS-16 radar tracking data. A direct comparison is possible because the measurements were made simultaneously by tracking the same effective target, which for the FPS-16 was metallic chaff in the balloon that carried the radiosonde transmitter.

With GMD measurements 10 times min^{-1} instead of the usual 1 min^{-1} and when elevation angles are $>10°$, the computed winds and ascent rates reproduced both the macroscale and mesoscale features derived from the FPS-16 data. The mesoscale features which have vertical wavelengths from 1.5–3 km include oscillations in wind direction and speed. When the elevation angles are $<10°$, the GMD antenna is misdirected by indirect signals reflected from the ground and large spurious oscillations and steps appear in the elevation angle measurements. It is impossible to recover the mesoscale winds from these erratic measurements, but the macroscale or synoptic scale winds can be obtained by fitting a low order polynomial to the entire set of low elevation angle measurements.

The winds computed from the FPS-16 measurements contain, between the earth's surface and the maximum altitude reached by the radiosonde balloon, many oscillations in wind speed and direction. The hodographs suggest that the velocities can be decomposed into a mean wind vector and a perturbation vector which rotates cyclonically or anticyclonically with height. In the stratosphere, anticyclonic rotation predominates. The perturbation vectors have magnitudes ranging from 0.5–10 m sec^{-1} and rotate through 2π rad in 0.5–3 km.

1. Introduction

Winds computed from radiosonde and rawin observations constitute the primary source of wind information for large-scale synoptic analyses. These winds, computed manually at the observation stations, contain components representative of the large-scale flow, but they also contain a mixture of oscillating components, some of which are real and some are spurious. When real, the oscillating components are representative of mesoscale features in the flow. When spurious, the oscillations are products of errors in the measurements, or errors and inconsistencies in the graphical methods of computation. The 2- and 4-min averaging used in the conventional computations tends to reduce all oscillations and reduce errors, but it cannot eliminate them; therefore, the result is a mixture that most closely approximates the large-scale flow.

Radars capable of tracking an airborne target with sufficient accuracy to provide resolution of both the large and mesoscale wind components are available but costly. Although they are too expensive to warrant general use in a meteorological network, they can be be used as standards in sumultaneous tracking experiments. With the aid of a standard, the potentials and limitations of the present rawin system can be determined.

The machine methods for processing GMD-1 rawin tracking data and radiosonde data which are discussed in this article were derived from a study of several radiosonde ascents made at Pt. Mugu, Calif. During each ascent, while the GMD-1 was tracking the radiosonde transmitter, an FPS-16 radar was tracking metallic chaff contained in the special radiosonde balloon.

From the FPS-16 measurements the accuracy of the thermodynamic height computations can be assessed in addition to an assessment of the accuracy of the GMD-1 measurements. Most important is the opportunity to test the potentials of the GMD equipment by comparing the computed winds to a reliable standard.

2. Definition of a standard

FPS-16 measurements. Every 0.1 sec the FPS-16 radar measures and records slant range to the nearest yard, and azimuth and elevation angles to the nearest 0.001°. The accuracy of these measurements has been reviewed by Scoggins (1963) who accepts the values quoted by Sanderlin of an rms accuracy of 5 yards in slant range and 0.01° in azimuth and elevation angles.

Evidence of random and periodic errors in the elevation angles are shown in Fig. 1 taken from a small

[1] Present affiliation: The University of Hawaii, Honolulu.

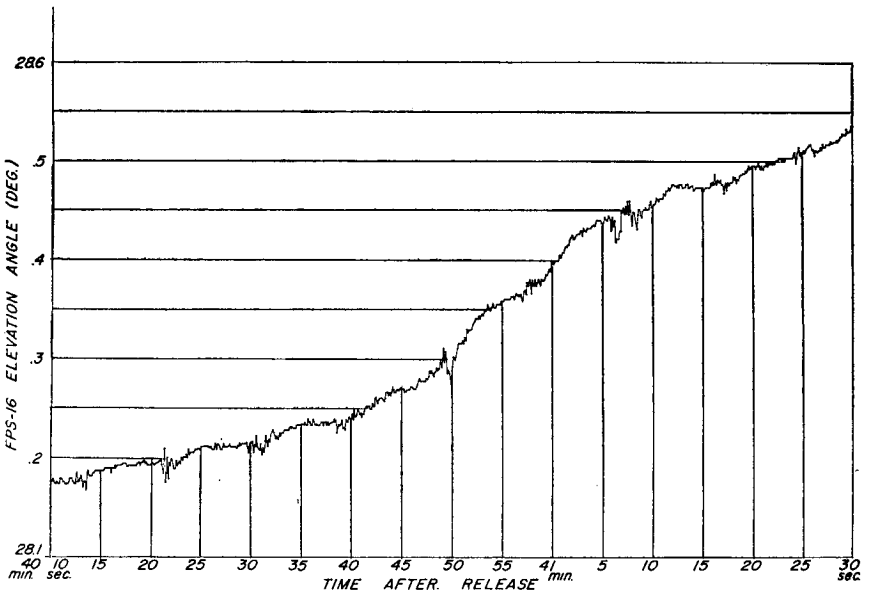

FIG. 1. Example of FPS-16 elevation angles, 7 February 1964.

segment of the data obtained during the ascent of 7 February 1964. The abscissa, which represents time after release, was divided into units of 5 sec beginning 40 min and 10 sec after release. The expanded ordinate scale, which spans only 0.5°, permitted accurate plotting to 0.001°. The observations were plotted as recorded every 0.1 sec. It is clear by inspection that the elevation angles contained periodic oscillations superimposed on a general increase. The period of the oscillations varied between 9 and 10 sec. Superimposed on these were high frequency random deviations, approximately 0.002°–0.003° in magnitude. Large spurious deviations, 0.01°–0.03° in magnitude, are also evident every 9 or 10 sec., i.e., at the same period as the above mentioned oscillations. These large errors, which appear to have been correlated with positive curvatures in the trace, obviously must be eliminated along with the smaller random deviations. It seemed desirable, however, to preserve the periodic oscillations to determine the magnitude of the speed oscillations they produce.

Method of processing FPS-16 data. After examining several graphs of this type, it was decided that a relatively simple method of processing the FPS-16 data would provide the desired standard. To remove the high frequency oscillations without introducing spurious frequencies, the arithmetic mean of every 10 consecutive non-overlapping points was computed. This generated 1-sec average values at intervals of 1 sec. Winds were then obtained by centered differencing.

Since winds were computed from azimuth angles and the distance of the balloon from the FPS-16 (measured on a curved earth), one might expect the resulting winds to differ, if 1) the distance was computed from the averaged values of range and elevation angle, or 2) the distances were first computed from the raw data and then averaged. A test was conducted to compare the results of both methods. Differences in the computed winds were insignificant and the second method was arbitrarily selected.

All calculations were made by a computer using the actual observations of slant range and angles. The height z above the observing radar and distance D over a curved earth were obtained from the formulae

$$z=R\left[\left\{1+\frac{2r}{R}\sin\epsilon+\left(\frac{r}{R}\right)^2\right\}^{\frac{1}{2}}-1\right], \tag{1}$$

$$D=R\theta=R\left[\cos^{-1}\left(\frac{\cos\epsilon}{1+z/R}\right)-\epsilon\right], \tag{2}$$

where R is the earth's radius, r the slant range, ϵ the elevation angle and θ the angle between radii from the center of the earth to the radar and to the balloon.

The vertical and horizontal velocities of the balloon were computed for the ith point by a finite differencing between the heights, times and horizontal positions at points $i+1$ and $i-1$. This provided 2-sec average velocities of the balloon at a 1-sec interval. To determine the horizontal velocity of the air, the velocities of the balloon relative to the air must be removed. The relative velocities were expected to be oscillatory with periods of the order of 5–15 sec. Therefore 10-, 20- and 40-sec average velocities were also computed by centered differencing and compared to the 2-sec average velocities. As before, the position coordinates were averaged without overlapping the data points but each average was now derived from 50, 100 and 200 consecutive points.

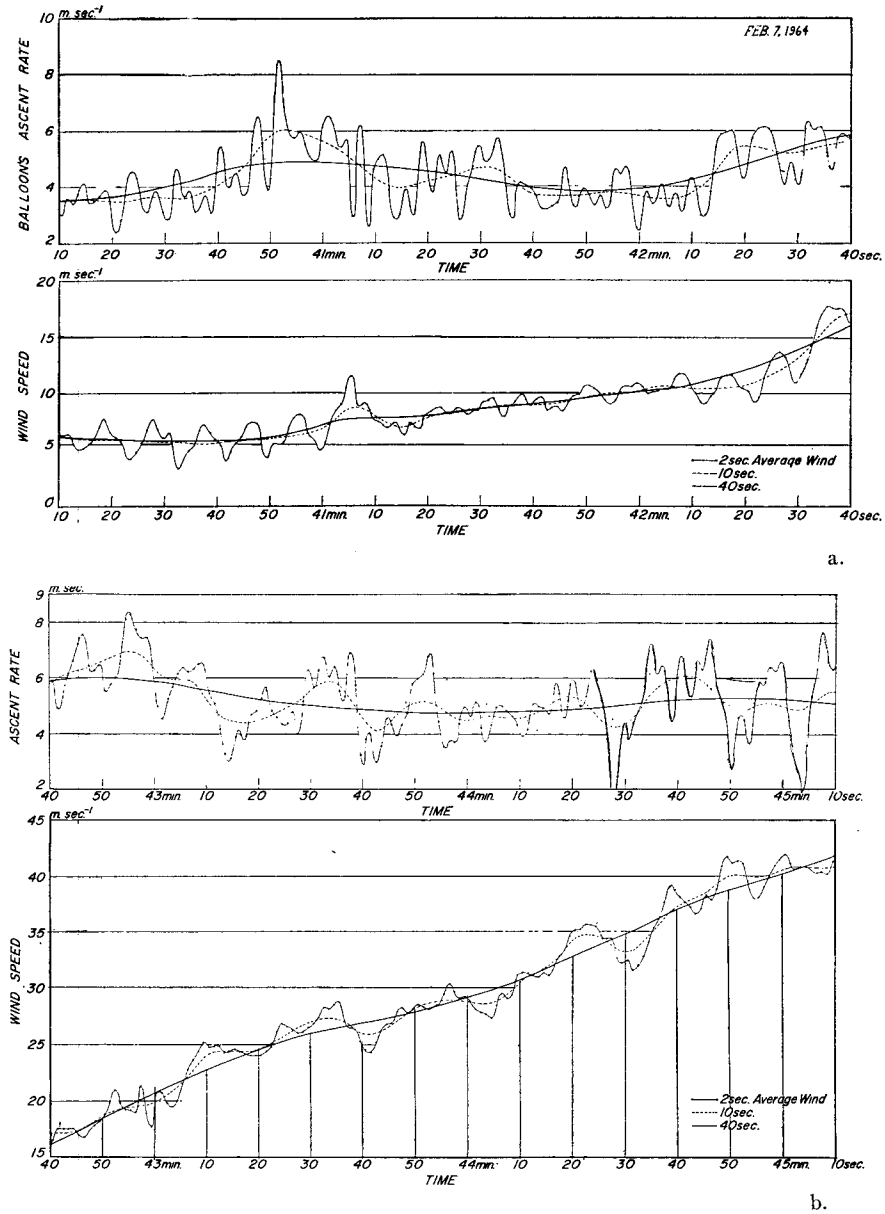

FIG. 2. FPS-16 wind speeds and ascent rates a., from 40 min 10 sec to 42 min 40 sec after release on 7 February 1964, and b., from 42 min 40 sec to 45 min 10 sec.

Examples of winds and balloon ascent rates. Examples of the velocities computed by the above methods from the FPS-16 data are presented in Figs. 2a and 2b. Consecutive in time, they represent a small portion of the 7 February ascent. In both figures, the upper graph depicts the ascent rate of the balloon, the lower graph delineates the horizontal speed of the balloon. The latter, with reservations, has been labeled "wind speed." Fig. 2a begins 40 min 10 sec after release, i.e., the same time as Fig. 1. The periodic oscillations which were evident in the elevation angles of Fig. 1 are clearly evident in the 2-sec average "wind speeds" of Fig. 2a. Oscillations of ± 2 m sec^{-1} with a period of about 9 sec characterize the first minute. During this time, the 10-sec average speeds (dashed line) and the 40-sec average speeds (heavy line) remained almost constant even though the elevation angle increased (Fig. 1). This implies an increase in the average ascent rate of the balloon. The upper graph confirms the increase from 3.5–6 m sec^{-1} for the 10-sec average and 3.5–5 m sec^{-1} for the 40-sec average.

It is interesting to note that the oscillations in the 2-sec averages about the 40-sec averages are approximately ± 2 m sec^{-1} for both the vertical and horizontal components. Symmetry in the magnitude of the oscillations would be expected if they represent the balloon's

motion relative to the air. Also, although it is not regular, there is approximately a $\pi/2$ phase shift between the respective components. The magnitudes, periods and phase shifts suggest they are produced by the balloon. For a discussion of the oscillations produced by ascending spherical balloons the reader is referred to a paper by Scoggins (1965).

If the assumption is correct that the high frequency oscillations are caused by accelerations of the balloon relative to the air, then they are effectively removed by the 40-sec averages and the latter are a measure of the wind speed. If, on the other hand, the oscillations are real wind variations, they can be treated only statistically. Therefore, in all subsequent examples the 40-sec average winds computed from the FPS-16 data shall be considered as the standard for comparing the GMD winds.

Additional support for the use of a 30- or 40-sec average as a standard was derived from a power spectrum of the 7 February FPS-16 winds. The time series of the 2-sec average wind speeds (4977 values) were analyzed for 500 lags. An outstanding feature of the spectrum was a large peak at 9 sec. This period, evident in the small sample of Figs. 2a and 2b, was predominant throughout the ascent. Again this suggests a natural period of the balloon. The power was a minimum between periods of 30 and 60 sec and remained relatively low up to 200 sec. The broad minimum implies that the averaging period could be increased to 200 sec, which is equivalent to averaging over a vertical distance of 1 km. As will be shown, this would resolve the macroscale or synoptic scale features of the wind but would obscure some mesoscale features which presently concern us.

3. Method of computing winds from GMD-1 data

Comparison of FPS-16 and GMD-1 measurements. Measurements of elevation angles contain the most troublesome errors in the GMD tracking data. An rms error of 0.05° is commonly accepted for both the GMD-1 and GMD-2 measurements of azimuth and elevation angles. This is 5 times the FPS-16 error discussed earlier. However, for estimating the accuracy of wind computations, an rms error may not be appropriate if the errors are occasionally large and organized rather than random. Errors of this type are evident in the GMD data.

In Figs. 3a and 3b, the GMD elevation angles are compared directly to the FPS-16 measurement. The left scale on the ordinate applies to the FPS-16 elevation angles. Two degrees plus the vertical displacement in the figures determine the GMD angles. This parallax difference is caused by a difference of 3363 yards between the locations of the GMD and the FPS-16 radar.

Between the 38th and 40th minute (Fig. 3a), when the elevation angles were approximately constant, the GMD measurements contain spurious deviations of about 0.05°, i.e., equal to the rms error. To significantly reduce these errors an average of 30 sec is required for the GMD measurements.

Between the 43rd and 45th minute (Fig. 3b), when the elevation angles were decreasing rapidly, the amplitude of the spurious deviations increased to ±0.1° and 0.2° or 2–4 times the rms error. Again the GMD measurements must be averaged over a 30- or 40-sec period to reduce the effects of these spurious oscillations. For nonoverlapping means, 5–7 consecutive measurements appear to be a lower limit for the averaging interval.

GMD-1 measurements and data reduction. A complete set of measurements in the GMD-1 system includes pressure, temperature, relative humidity, azimuth angle, elevation angle and time. The azimuth and elevation angles are printed on a tape every 0.1 min. Included in the printout are the angles in degrees and a portion of the vernier scale which can be read to the hundredths of a degree. To synchronize the tracking and thermodynamic data, the latter can be determined at the same times as the former, or the thermodynamic data can be read independently if the time of each reading is determined. The second method is preferred because the pressure is calibrated only when the baroswitch is activated at the completion of each temperature contact. For maximum accuracy, the baroswitching should also activate a timer. Since a timer is not included in the GMD equipment, it was necessary to assume that the time between contacts was determined by the corresponding distances on the radiosonde recorder chart. This assumption is valid if the line voltage is constant, for then the recorder chart feeds out at a constant rate.

All the necessary charts for the Pt. Mugu soundings were available. Pressures were read to the nearest millibar from the calibration charts. Frequencies corresponding to temperature and relative humidity were read to the nearest tenth of an interval from the recorder charts; this provides temperature measurements accurate to the nearest 0.1–0.2C. Times were read to 0.01 min.

In the course of this study it was found that the pressure calibration chart could not be accepted literally. Friction in the baroswitch apparently produces errors in the pressure calibration. The sandwich of conductors and insulators in the baroswitch does not have a smooth surface. If the needle point on the baroswitch arm (activated by the pressure-sensing aneroid) encounters a surface irregularity, it might be held until a pressure difference develops to overcome the friction. The pressure difference would, of course, represent an error. Apparently, this friction-induced error is less probable when the instrument is swinging and bouncing in flight, because observed errors in the derived ascent rates were removed by smoothing the pressure differences between successive contacts. The smoothing also removed round-off errors in reading the pressure calibration chart at low pressures. When the pressure increment between contacts is less than 1 mb, the reading error is of the

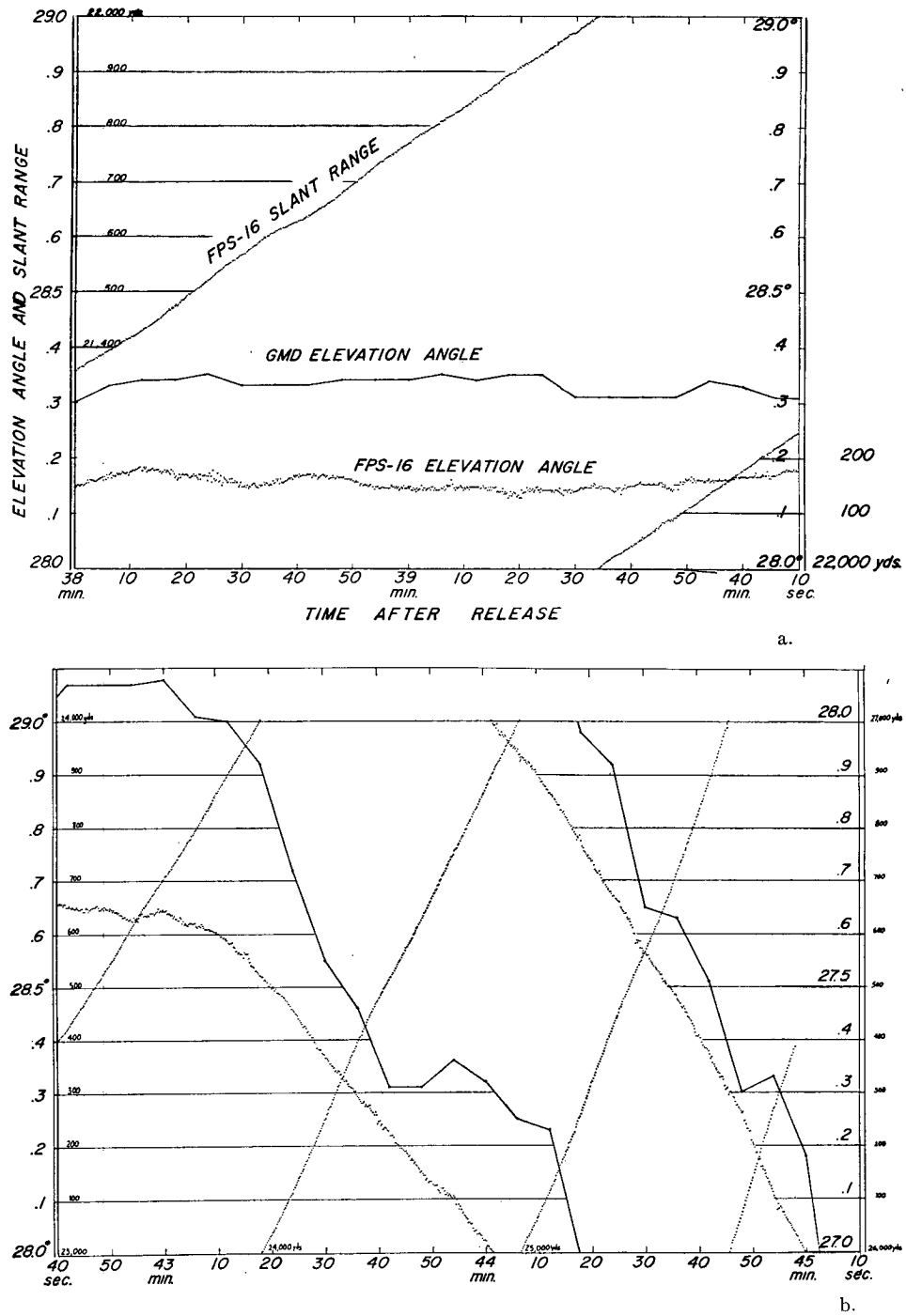

FIG. 3. Comparison of GMD and FPS-16 elevation angles a., 38 min to 40 min 10 sec after release 7 February 1964, and b., 42 min 40 sec to 45 min 10 sec.

same magnitude as the pressure increment itself. In addition, it was necessary to smooth the series of contact times. Errors in the timing were probably caused by non-uniform line voltages. All smoothing was done objectively as part of the computer program to be discussed next.

Computational methods. In the GMD-1 rawin system the pressure contacts provide the most natural interval for processing the data. By choosing the pressure contact interval as the basic interval, the thermodynamic data is specified with no interpolations. However, the time interval between contacts is not a constant, but increases as the pressure decreases. It is about 0.5 min near the earth's surface and increases to approximately

1 min at 100 mb and to 1.5 min at 50 mb. If the pressure contact interval is used for computing winds as well as for specifying thermodynamic quantities, the number of observations of azimuth and elevation angle that enter each wind calculation will vary. The number varies from 5 or 6 observations per interval near the surface of the earth to about 10 or 15 at 50 mb. Since the errors in the computed heights and in the observed elevation angles also tend to increase as the pressure decreases, averaging between the pressure contacts automatically tends to compensate for the degeneration of the data. The number of values that enters the average near the ground is also consistent with the minimum required to remove spurious oscillations as discussed in the previous section.

An arbitrary decision was made to obtain winds at the mid-point of the interval between successive contacts (to be referred to simply as "mid-points"). All measurements of azimuth angle and elevation angle between successive contacts were averaged and the mean value was assigned to the mid-point. The time and the height of the mid-point were taken to be the arithmetic means of the times and heights at the bracketing contacts. The distance out over a curved earth was computed from the mid-point height and the average elevation angle. Then the distance out and the average azimuth angle were used to compute horizontal winds by finite centered differences.

The computer program to process the GMD radiosonde data involves the following steps:

1) editing the data to remove gross errors due to transcription or key-punching mistakes;
2) filtering the data to remove random noise;
3) computing the winds and their shears; and
4) checking the shears on the basis of physical credibility.

At the conclusion of the fourth step, the program either terminates by printing out the resultant information or recycles to step 2) where a more powerful filtering device is applied to the data.

Thermodynamic quantities are processed first. To remove irregularities in the GMD chart feed speed, the recorded time of each contact is smoothed by two applications of a 3-point average in which all points are weighted equally. To remove calibration errors and roundoff errors, the same 3-point average is applied 6 successive times to the pressure data. No smoothing is applied to the temperature or humidity data.

The height of each contact above the earth's surface is computed by a stepwise application of the integrated hydrostatic equation between the smoothed pressure limits of successive contacts. In the integration, virtual temperature is assumed to vary as $p^{0.286}$ between contacts. The heights are stored then the distances out and average azimuth angles are computed and stored for the wind computations.

At each mid-point the ascent rate of the balloon and the horizontal wind vector (direction and speed) is computed by finite differencing between the position coordinates at the adjacent mid-points. These two contact interval averages correspond to about a 1-min average near the surface and a 3-min average at 50 mb.

As part of the computer program, averaging of the basic data for the mid-points is increased from 1 to 3 contact intervals when the following criterion is exceeded at more than one consecutive mid-point:

$$[(u_3+u_1-2u_2)^2+(v_3+v_1-2v_2)^2]^{\frac{1}{2}}\geq 4 \text{ m sec}^{-1},$$

where u and v are the wind components and the subscripts identify consecutive mid-points. This criterion which limits the magnitude of the second difference of the wind vector rejects most oscillations due to errors. Using the new averages the computer again calculates at each mid-point the wind and the second difference. If the criterion is still exceeded, a low-order polynomial is fitted to the erratic data to recover the macroscale winds. A further increase in the averaging interval merely spreads out and phase shifts the errors. The mesoscale oscillations are therefore lost in the noise.

4. Comparison of FPS-16 and GMD-1 ascent rates and winds

Ascent rates: When ascent rates are compared, two completely independent sets of measurements are involved. The FPS-16 rates were computed from tracking data, the GMD rates from thermodynamic data. The time intervals are also independent since the FPS-16 measurements were made at 0.1-sec time intervals whereas the GMD data were obtained at a variable time interval determined by the baroswitch contacts.

The excellent agreement shown in Fig. 4 between the two ascent rates computed from the 7 February 1964 data attests to the accuracy of the radiosonde data. Only above 13 km do significant deviations occur. These errors are attributed to the pressure calibration because they were much greater before the contact pressures were smoothed (note unconnected crosses).

On the other hand, the errors in the ascent rates on 20 February 1964 are predominantly a shift of phase. These shifts are attributed to a non-uniform chart speed (non-uniform line voltage) which introduces an error in the contact times.

Both diagrams dramatically illustrate why it is dangerous to assume a constant ascent rate for a radiosonde balloon. It is standard practice to assume a constant rate between the pressure reference contact, i.e., between every 5 contacts. This corresponds to 5 consecutive points on the dashed GMD-1 line. In 5 points, the ascent rate frequently varied from 4–6 m sec^{-1} or about 150%. An extreme case occurred between the 3rd and 5th minute on 20 February where the rates varied 600%. Errors in winds caused by the assumption

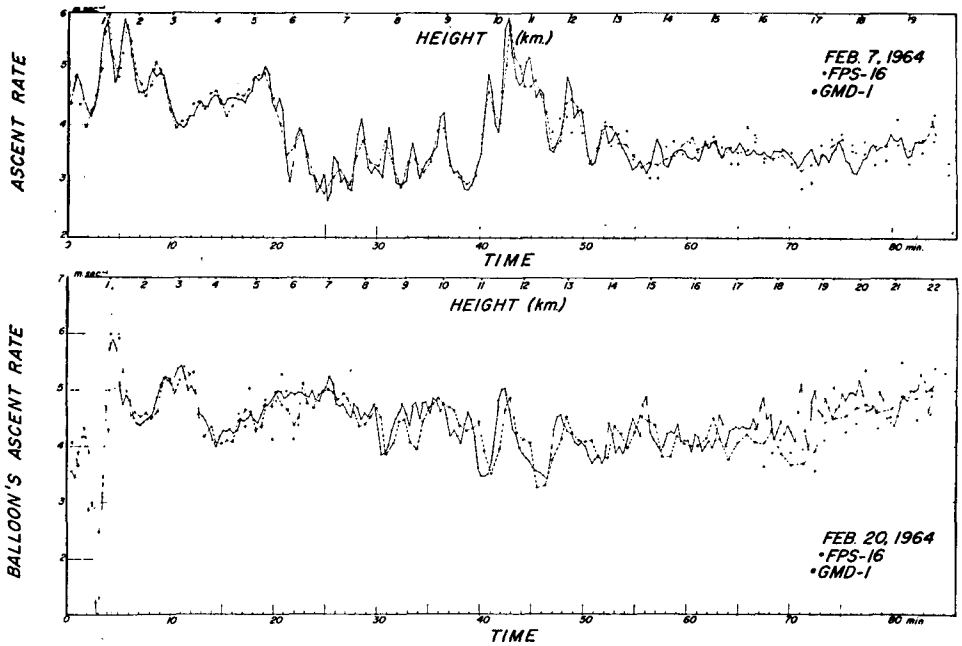

FIG. 4. Balloon ascent rates, 7 February and 20 February 1964. Solid line FPS-16; dashed line GMD.

of a uniform ascent rate have been discussed by Danielsen (1959).

Wind profiles and hodographs. Ascent on 7 February 1964. Wind speeds derived from the 7 February data are presented in Fig. 5a. The profile is unusual because the large-scale features include three maxima. The first is at an elevation of 1 km; the second, 6 km; and the third, the main jet, is centered at 11.6 km. Superimposed on these macroscale features are numerous mesoscale and microscale oscillations in the wind speed. In this report, the term mesoscale will refer to wind oscillations with a vertical wavelength greater than 1 and less than 3 km, as for example, the oscillations between 14 and 16 km. The term microscale will apply to all shorter wavelengths such as those between the 7th and 10th kilometer. It is clear in Fig. 5a that the GMD winds reproduce both the macroscale and mesoscale features of the wind profile from the surface to 19 km. Within this interval only the microscale features were distorted or eliminated. Since the two pro-

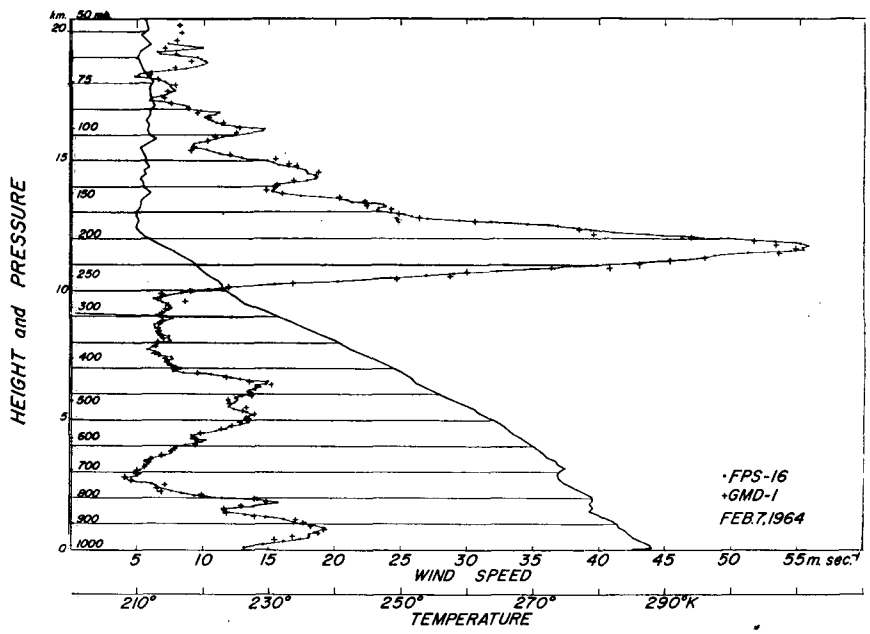

FIG. 5a. Wind speed and temperature profiles, 7 February 1964.

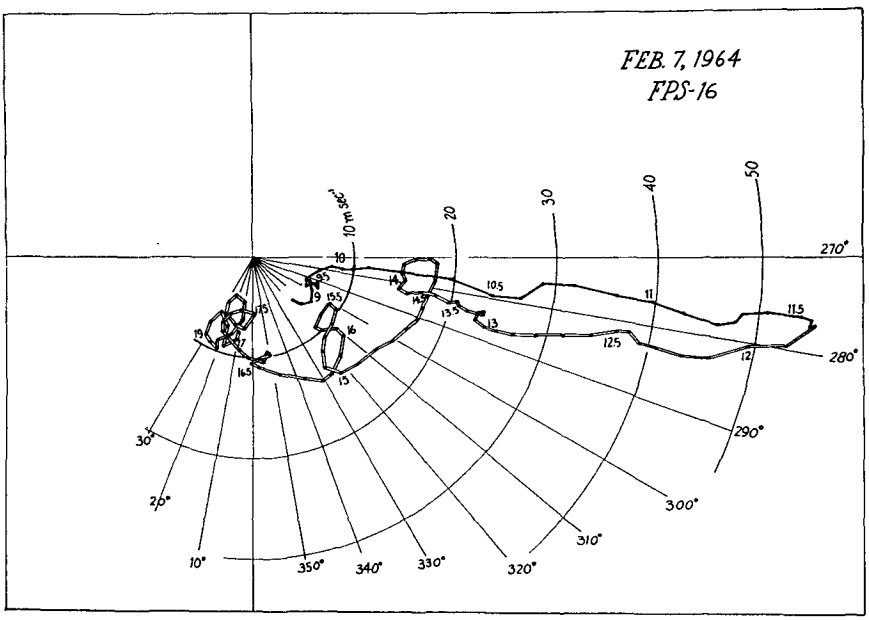

FIG. 5b. FPS-16 wind velocity hodograph, 7 February 1964.

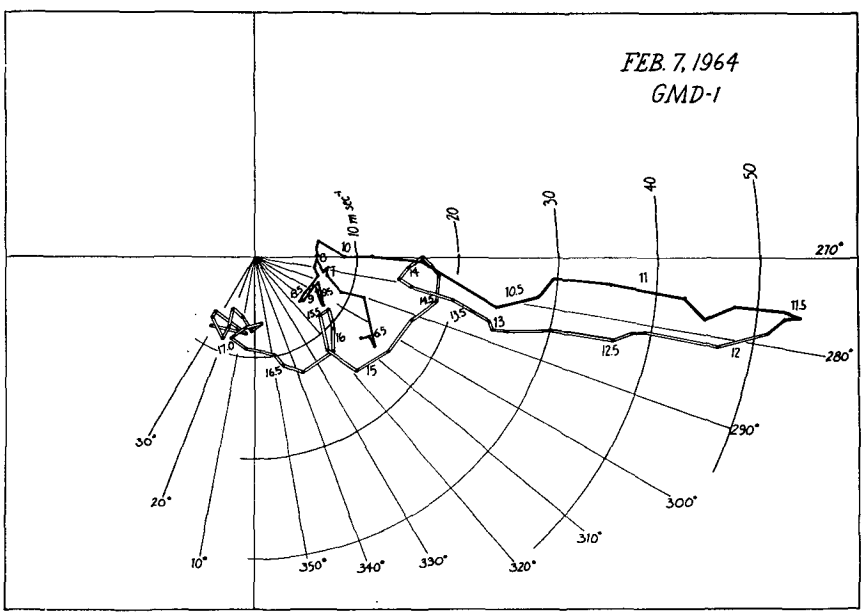

FIG. 5c. GMD-1 hodograph, 7 February 1964.

files were computed from completely independent sets of measurements, there can be little doubt about the existence of both the macroscale and mesoscale features. Also, the mesoscale oscillations above the jet are similar to those reported by Barbe (1958), Sawyer (1961) and Scoggins (1965).

A comparison of Figs. 5a and 5b shows that oscillations in the wind speed correlate with oscillations in wind directions, i.e., the oscillations at 10.5 and 11.2 km correspond to undulations in the hodograph. The mesoscale speed oscillations at 14 and 16 km also correspond to loops in the hodograph. Note, in particular, that the loop at 14 km was produced by an anticyclonic turning of the wind vector with height.

The undulations and loops in the FPS-16 hodograph are also evident in the GMD hodograph (Fig. 5c). There is, of course, some distortion in the mesoscale features of the GMD hodograph but all significant features are identifiable. Considering the many sources of error in the GMD rawin and radiosonde data, the ac-

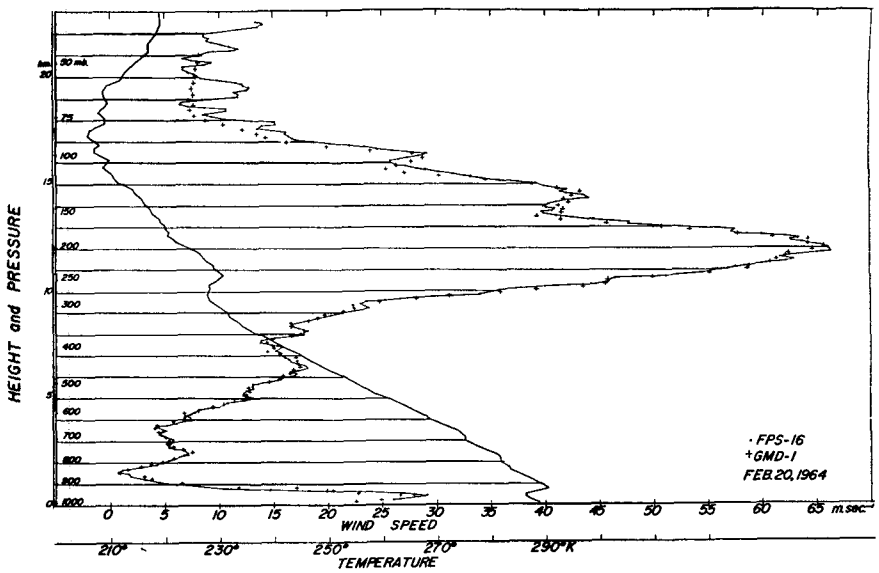

FIG. 6a. Wind speed and temperature profiles, 20 February 1964.

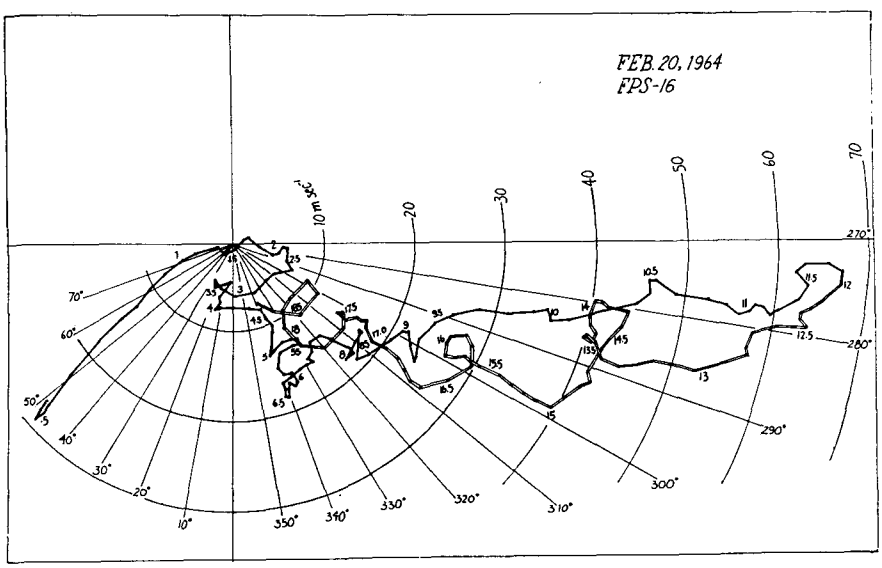

FIG. 6b. FPS-16 wind velocity hodograph, 20 February 1964.

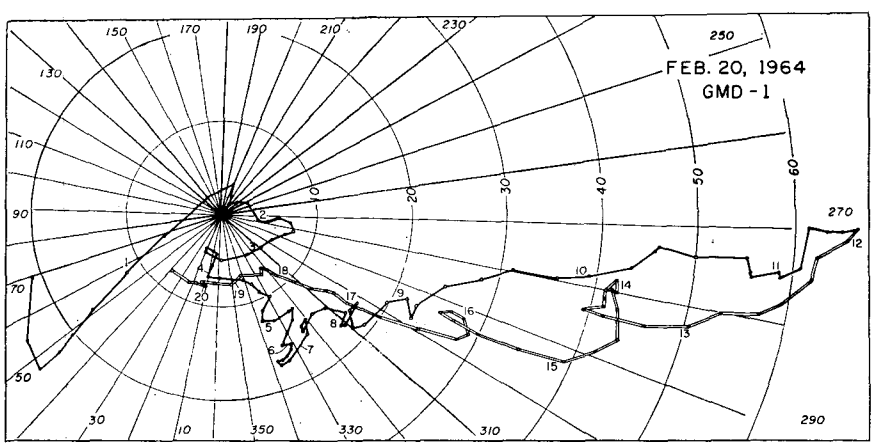

FIG. 6c. GMD-1 hodograph, 20 February 1964.

curacy of the vector winds is quite good. With few exceptions, the wind speeds are accurate to within ± 1 m sec^{-1} and the wind directions to within $\pm 2°$. The maximum error in speed at an isolated point is 2 m sec^{-1} and the maximum error in wind direction is $\pm 5°$.

Ascent on 20 1964. The wind speed profile for 20 February (Fig. 6a) contains two maxima. The first maximum of 28 m sec^{-1} at 0.05 km presents the downslope Santa Anna wind. In the next kilometer, the speeds decrease rapidly to almost zero. Above this level the wind speeds increase to a strong jet of 67 m sec^{-1} at 12 km then decrease to a minimum of 10 m sec^{-1} at approximately 19 km. Once again, numerous mesoscale and microscale oscillations are superimposed on the mean profile. From the surface to 13 km, the GMD wind speeds correspond closely to the FPS-16 wind speed profile, but above this level, errors of 3 and 4 m sec^{-1} are evident. These errors distort the mesoscale oscillation at 14 km and displace the minimum at 16 km to a slightly lower level. Above the 17-km level, the increasing number of data points which enter the averages in the GMD-1 calculations completely smooth out the mesoscale oscillations. One notices, however, that the mean GMD speeds are consistently lower than the mean of the FPS-16 measurement. If the reader refers back to Fig. 4, he will notice that the ascent rate calculated from the GMD data was slower than that of the FPS-16 between 17 and 20 km. The corresponding errors in ascent rate and speed are probably caused by a faster than normal feedout rate of the recorder chart. The chart intervals between successive contacts is then overestimated and the speed underestimated. However, some of the errors can be attributed to errors in measurements in elevation angles, for the accuracy of the elevation angle measurements degenerates as the elevation angles decrease. Since the mean wind speed on 20 February was greater than that of 7 February, generally lower elevation angles were encountered.

Hodographs prepared from the FPS-16 winds (Fig. 6b) and the GMD winds (Fig. 6c) contain zig-zags, undulations and loops. Notice that the loops in the FPS-16 hodograph at 14, 16 and 18.5 km all correspond to anticyclonic rotations. The two hodographs correspond closely below 12 km, but at higher elevations the mesoscale loops are distorted and damped by the 3-contact interval smoothing. Loss of the mesoscale loops does not seriously degrade the macroscale winds. A smooth curve drawn through the FPS-16 hodograph would approach the GMD hodograph.

Errors in wind speed at very low elevation angles. In the examples just presented, the method for computing winds from the GMD data proved to be highly satisfactory. However, in both cases, the elevation angles were never less than 10°. An example will now be presented which illustrates the breakdown of the method when the elevation angle was very low. At 0043 GMT 7 March 1964, the average wind speeds were quite high, as shown in Fig. 7. The GMD winds agreed with the FPS-16 winds up to 3 km. Above this level the GMD winds were 4–6 m sec^{-1} slower than the FPS-16 winds. Above the 8-km level, errors as great as 25 m sec^{-1} were produced by the GMD data. The profile in Fig. 7 represents the speeds computed from data averaged over 3 contact intervals. The initial winds contained still larger errors.

Clearly, these results are unacceptable. Increasing the averaging interval to 5 and 7 contact intervals pro-

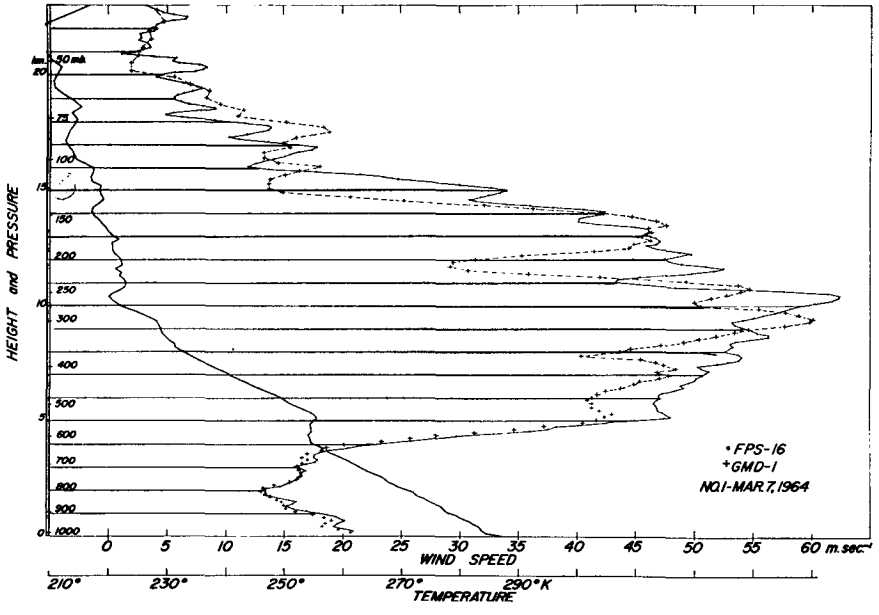

FIG. 7. Wind speed and temperature profiles, 7 March 1964.

duced no substantial improvements. The larger interval reduced the magnitude of the speed errors, but spread them over more points and introduced phase shifts. It was therefore considered necessary to examine the elevation angles in detail to determine the characteristics of the errors and then to attempt other methods of smoothing which might at least preserve the mean wind speeds.

5. Determination of errors in GMD elevation angles

A direct comparison of the elevation angles measured by the GMD with those measured by the FPS-16 is complicated by the difference in the elevation angle produced by parallax. The effect of parallax can be removed, however, by simply transforming the FPS-16 measurements over to the position of the GMD-1 rawin system. In the transformation equations, the curvature of the earth can be neglected because this produces an error of approximately 0.02°, which is neglibile in comparison to the GMD errors.

The equations relating the azimuth and elevation angles which would be measured at the GMD site to the azimuth and elevation angles measured by the FPS-16 are as follows:

$$D_G^2 = D_F^2 + D_{GF}^2 - 2D_F D_{GF}\cos\Delta\alpha, \tag{3}$$

$$\Delta\alpha = \alpha_R - \alpha_F, \tag{4}$$

$$\epsilon_G = \tan^{-1}\left(\frac{D_{GF}}{D_G}\tan\epsilon_F\right), \tag{5}$$

$$\alpha_G = \alpha_F - \sin^{-1}\left(\frac{D_{GF}}{D_G}\sin\Delta\alpha\right), \tag{6}$$

where

D_G is the horizontal distance between the balloon and the GMD,

D_F is the horizontal distance between the balloon and the FPS-16,

D_{GF} is the horizontal difference between the GMD and the FPS-16,

α_G is the azimuth angle to the balloon at the GMD site,

α_F is the azimuth angle to the balloon at the FPS-16 site,

α_R is the azimuth angle to the GMD at the FPS-16 site,

ϵ_G is the elevation angle of the balloon at the GMD site, and

ϵ_F is the elevation angle of the balloon at the FPS-16 site.

Errors in the elevation angles measured by the GMD system during the ascent of 7 February were relatively small. They were predominately negative during the early portion of the run and predominately positive during the latter portion of the run. The change from negative to positive departures was associated with a change from large to small azimuth angles and was probably due to a small tilt in the GMD-1 radar antenna. Although the rms error was only slightly greater than 0.05°, there were certain periods when the errors were organized to form long-period oscillations.

During the ascent of 20 February 1964 the errors remained small until the elevation angles descreased to 12°. Between 12° and the minimum of 10.4° the errors were predominantly positive with oscillations from 0°

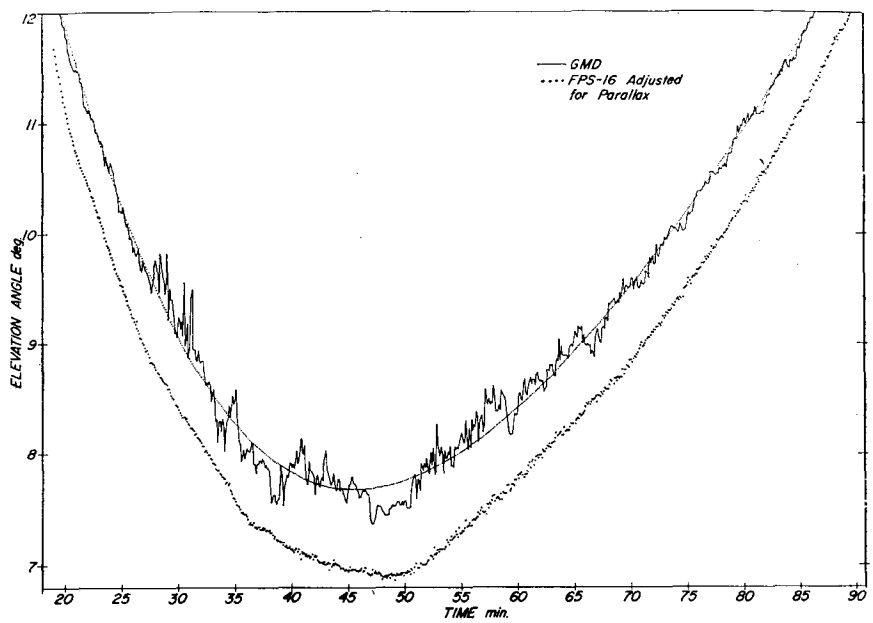

FIG. 8. GMD and parallax-adjusted FPS-16 elevation angles plus fourth-order polynomial, 7 March 1964.

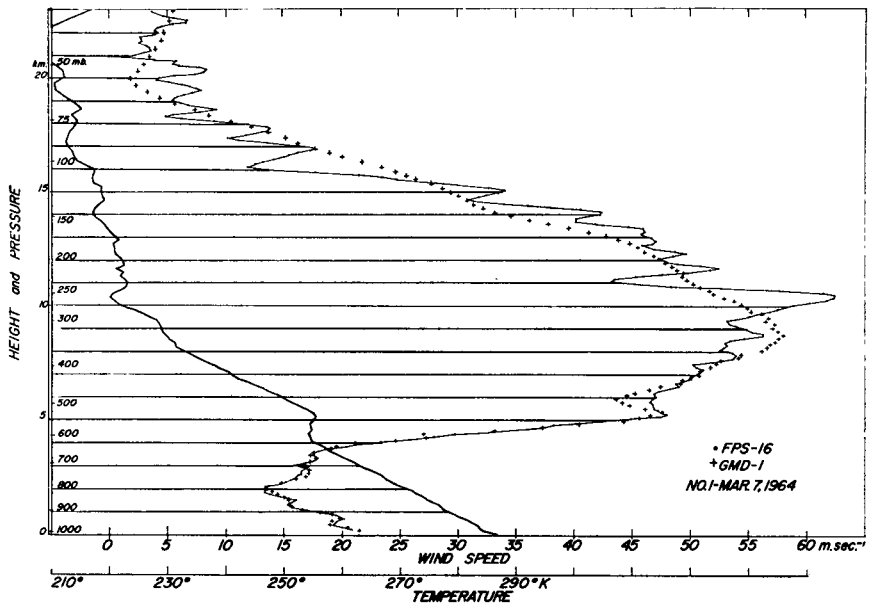

FIG. 9a. Recomputed wind speed and temperature profiles, 7 March 1964.

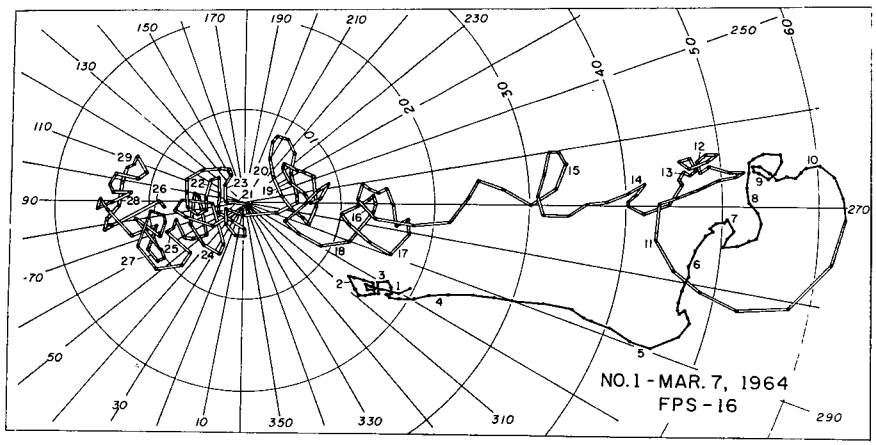

FIG. 9b. FPS-16 hodograph, 7 March 1964.

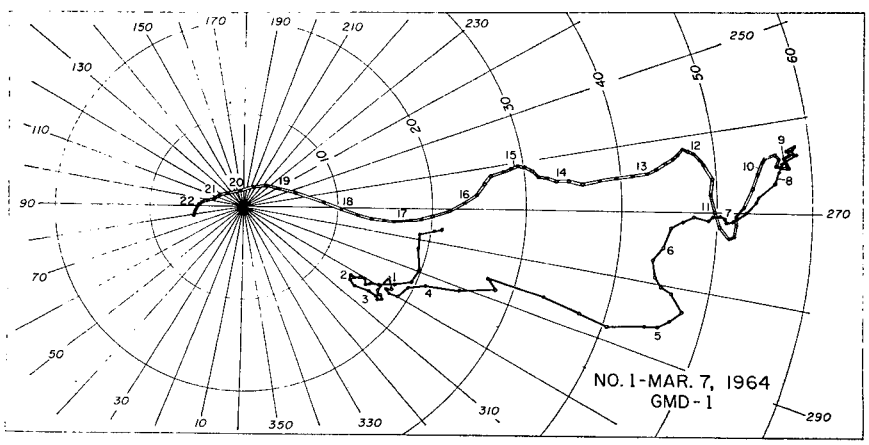

FIG. 9c. GMD-1 hodograph, 7 March 1964.

to 0.2° and 3–5 min periods. The FPS-16 angles produced a much smoother curve with random ±0.03° fluctuations.

A more extreme example which accounts for the wind errors in the 7 March ascent is presented in Fig. 8. The FPS-16 measurements, only every 60th observation is plotted, produce a relatively smooth curve compared to the erratic GMD curve. When $\epsilon<10°$ the GMD curve deviates 0.3°–0.7° from a smooth curve and the deviations are predominantly of the same sign for 3–7 min periods. The combination of large amplitudes and long periods makes it impossible to recover the proper smooth curve by averaging over discrete intervals or by using running averages. However, a low-order polynomial fitted to the entire set of measurements as the fourth order curve shown in Fig. 8, does approximate the FPS-16 curve. The fourth order was selected by testing the rms deviations as the order of Gram-Schmidt polynomials was increased from 3 to 10. These particular polynomials were used because they are orthogonal for a discrete set of points. In this case the rms deviation decreased from 0.27° at order 3 to 0.14° at order 4 to 0.11° at order 5. From order 5 to 10 the rms deviation remained >0.10°.

Another source of error for the 7 March winds is evident in Fig. 8. A systematic error of 0.69° in the GMD elevation angle measurements pervades the entire run. Since this error did not change with azimuth angle it is a calibration, not a leveling error. A similar error was noted for an ascent made 12 hr later, but it was absent on a third ascent made 6 hr after the second. The effect of this positive error increases as ϵ decreases but it systematically leads to slower speeds.

Mean winds from polynomial method. The winds for 7 March 1964 were recomputed after the systematic error of 0.69° was removed. Averages over a 1-contact interval were used up to 8 km. Averages over 5 contact intervals were used above 6.5 km with the elevation angles given by the polynomial. In the 1.5-km overlap, the winds were blended to provide a smooth transition.

The resulting wind speeds (Fig. 9a) approximate the running mean of the FPS-16 winds above 8 km. Occasionally, the GMD winds differed by 10 m sec^{-1} from the mean winds but the average error is ≃2 m sec^{-1}. Considering the large errors in the measured elevation angles, this recovery of the mean wind profile is quite satisfactory. Of course, the mesoscale oscillations in the FPS-16 profile have been lost in the noise and, as a consequence, the jet in the GMD winds is 1.5 km beneath the maximum wind in the FPS-16 profile. In this case the maximum wind is produced by a mesoscale oscillation above the mean jet.

Evidence to support this interpretation is found in the FPS-16 hodograph in Fig. 9b. Between 9 and 12 km, a large-amplitude anticyclonic loop is formed by an anticyclonically rotating perturbation vector of 10 m sec^{-1} amplitude. At higher elevations, anticyclonic loops predominate but the amplitudes are 2–4 m sec^{-1} as they were in the February ascents.

The smooth curve of the GMD hodograph (Fig. 9c) is more conventional and approximates a mean curve through the looping FPS-16 hodograph. It is obvious that these mesoscale loops are not representative of the large-scale motions depicted in synoptic analyses and for this reason they should be removed or filtered from the wind profiles and hodographs unless a detailed mesoscale analysis is required. The present method of computing winds neither resolves nor removes these mesoscale oscillations which leads to considerable confusion concerning the accuracy of the winds and the capabilities of the GMD rawin system.

6. Conclusions

A comparison of the vector winds computed from GMD-1 and FPS-16 tracking data indicates that both the macro- and mesoscale features of the wind are accurately resolved from the GMD data if the observations are made 10 times per minute and the elevation angles are >10°. When the above conditions were met and the GMD-antenna was properly leveled, the GMD-1 winds, with few exceptions, were accurate to ±1° and ±1 m sec^{-1}.

At lower elevation angles interference by ground reflected signals produces large errors in the measurements of elevation angle. The errors frequently maintain the same sign for several minutes which makes it extremely difficult or impossible to recover the proper curve of elevation angles by smoothing the data. However, by fitting low-order orthogonal polynomials to the complete set of low-angle measurements, a close approximation to the macroscale winds can be obtained. These mean winds are comparable to those obtained by solving the balance equation from synoptic analyses of the geopotential fields; therefore, they are appropriate to conventional synoptic analysis.

Acknowledgments. This study was supported by the Aerospace Environment Division, NASA, Marshall Space Flight Center. The FPS-16 and GMD-1 data were supplied by the Inter-Range Instrumentation Group-Meteorological Working Group.

REFERENCES

Barbe, G. D., 1958: Donnés sur le vent en altitude. *J. Sci. Météor.*, **10**, 47–62.

Danielsen, 1959: The laminar structure of the atmosphere and its relation to the concept of a tropopause. *Arch. Meteor., Geophys., Bioklim.*, **A11**, 293–332.

Sawyer, J. S., 1961: Quasi-periodic wind variations with height in the lower stratosphere. *Quart. J. Roy. Meteor. Soc.*, **87**, 24–33.

Scoggins, J. R., 1963: An evaluation of detailed wind data that is measured by the FPS-16 radar/spherical balloon technique. NASA Tech. Note TN D-1572, 30 pp.

——, 1965: Spherical balloon wind sensor behavior. *J. Appl. Meteor.*, **4**, 139–145.